Design of fluid viscous dampers for optimal life cycle cost

I. Gidaris , A. Taflanidis
University of Notre Dame, Department of Civil Engineering and Geological Sciences

SUMMARY:
Probabilistic approaches for comprehensive cost–effective design of viscous dampers for seismic hazard mitigation are gaining increasing attention within the engineering community, especially in the context of retrofitting strategies. A probabilistic framework is presented here that allows for explicit consideration in the design process of (i) all important nonlinearities for both the dampers and the structural behavior, as well as of (ii) all important sources of uncertainty related to the seismic hazard. The framework is based on an assembly-based vulnerability approach for estimating earthquake losses and on stochastic ground motion models for describing the earthquake hazard. The life-cycle repair cost is quantified by its expected value over the space of the uncertain parameters for the structural and excitation models, and is estimated through stochastic simulation. For the design-optimization an algorithm appropriate for costly global optimization problems is adopted. An illustrative example is presented that shows the efficiency of the proposed methodology.

Keywords: fluid viscous dampers, life cycle cost optimization, robust performance based seismic design

1. INTRODUCTION

Probabilistic approaches for comprehensive cost–effective design of viscous dampers for seismic hazard mitigation are gaining increasing attention within the structural engineering community, especially in the context of retrofitting strategies. A realistic treatment of such a design requires proper integration of (i) methodologies for treating the uncertainties related to the seismic hazard over the entire life–cycle of the building, (ii) tools for evaluating the performance using socioeconomic criteria, as well as (iii) algorithms appropriate for stochastic analysis and optimization. This work uses a simulation based framework that addresses all important challenges associated with these steps for the design of fluid viscous dampers for retrofitting of building structures. A probabilistic foundation is used to address the various sources of uncertainty and quantify the expected life-cycle cost which is comprised by the lifetime repair cost of the structure due to expected future seismic losses and the upfront cost of the damper devices. This is established by characterizing the relative plausibility of different properties of the system and its environment (representing future excitations) by probability models. An assembly based vulnerability approach is used to estimate the repair cost due to losses of future seismic excitations and a realistic probabilistic model is presented for the latter that also addresses the potential of the ground motion exhibiting forward directivity effects. In this probabilistic setting, stochastic simulation is adopted for estimating the life-cycle repair cost. Though robust, this choice makes the associated design-optimization challenging, as it involves a large computational burden. To alleviate this burden, an efficient algorithm belonging in the greater family of Costly Global Optimization (CGO) search techniques is adopted. For illustrating this approach an example is presented that considers the optimal performance-based design of fluid viscous dampers for a three-story concrete structure.

2. PROBABILISTIC QUANTIFICATION OF LIFE-CYCLE COST

For evaluation of seismic cost adoption of appropriate models is needed for the structural system itself, the earthquake excitation and loss evaluation (Figure 2.1). The combination of the first two models provides the structural response and in the approach adopted here this is established in terms

of nonlinear time-history analysis. The loss evaluation model quantifies, then, earthquake performance in economic terms based on that response. The characteristics of these models are not known with absolute certainty. Uncertainties may pertain to (i) the properties of the structural system, for example, related to stiffness and damping characteristics; to (ii) the variability of future seismic events, i.e. the moment magnitude or the epicentral distance; to (iii) the predictive relationships about the characteristics of the excitation given a specific seismic event, for example duration of strong ground motion or peak ground acceleration; or to (iv) parameters related to the performance of the system, for example, thresholds defining fragility of system components. A probabilistic logic approach provides a rational and consistent framework for quantifying all these uncertainties through the entire life-cycle of the structure. In this approach, probability can be interpreted as a means of describing the incomplete or missing information about the system under consideration and its environment, representing the seismic hazard, through the entire life cycle. This leads ultimately to a design framework that can realistically and explicitly address all uncertainties involved in the modeling of the structure and its environment.

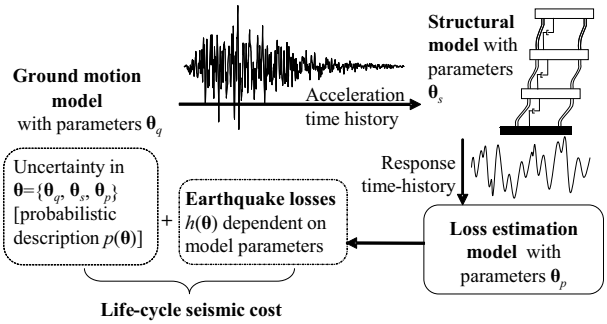

Figure 2.1. Augmented system model

In this setting, consider a structural system that includes some controllable parameters that define the system design, referred to herein as design variables, $\boldsymbol{\varphi} = [\varphi_1, \varphi_2, ..., \varphi_{n_\varphi}] \in \Phi \subset \mathbb{R}^{n_\varphi}$, where Φ denotes the bounded admissible design space. For the application discussed here, $\boldsymbol{\varphi}$ consists of the design characteristics of the fluid viscous dampers. Let $\boldsymbol{\theta} \in \Theta \subset \mathbb{R}^{n_\theta}$, denote the augmented vector of model parameters where Θ represents the space of possible model parameter values. Vector $\boldsymbol{\theta}$ is composed of all the model parameters for the individual structural system, excitation, and performance evaluation models indicated in Figure 2.1. For addressing the uncertainty in $\boldsymbol{\theta}$ a probability density function (PDF) $p(\boldsymbol{\theta})$, is assigned to it, quantifying the relative likelihood of different model parameter values. This PDF incorporates our available knowledge about the structural system and its environment into the respective knowledge, and should be selected based on this knowledge (Jaynes, 2003). The favorability of the system response, given the values of the model parameters, is evaluated by the risk consequence measure $h(\boldsymbol{\varphi}, \boldsymbol{\theta}) : \mathbb{R}^{n_\varphi \, x \, n_\theta} \to \mathbb{R}^+$, representing the expected utility from a decision-theoretic point of view:

$$h(\boldsymbol{\varphi}, \boldsymbol{\theta}) = C_{in}(\boldsymbol{\varphi}, \boldsymbol{\theta}) + C_{lif}(\boldsymbol{\varphi}, \boldsymbol{\theta}) \tag{2.1}$$

where $C_{in}(\boldsymbol{\varphi}, \boldsymbol{\theta})$ corresponds to the initial cost and $C_{lif}(\boldsymbol{\varphi}, \boldsymbol{\theta})$ to the additional cost over the lifetime of the structure. The expected life-cycle cost $C(\boldsymbol{\varphi})$ is then simply given by:

$$C(\boldsymbol{\varphi}) = E_{\boldsymbol{\theta}}[h(\boldsymbol{\varphi}, \boldsymbol{\theta})] = \int_{\Theta} h(\boldsymbol{\varphi}, \boldsymbol{\theta}) \, p(\boldsymbol{\theta} \mid \boldsymbol{\varphi}) d\boldsymbol{\theta} \tag{2.2}$$

where $E_{\boldsymbol{\theta}}[.]$ denotes expectation with respect to the PDF for the model parameter vector $\boldsymbol{\theta}$. The life-cycle cost design problem requires determination of the optimal design parameters $\boldsymbol{\varphi}^*$:

$$\boldsymbol{\varphi}^* = \arg\min_{\boldsymbol{\varphi}\in\mathbb{R}^{n_\varphi}} \left\{ C(\boldsymbol{\varphi}) \mid \mathrm{f}_c(\boldsymbol{\varphi}) \geq 0 \right\} \tag{2.3}$$

where $f_c(\boldsymbol{\varphi})$ is a vector of deterministic constraints, related, for example, to location or space constraints for the dampers. Note that in this formulation, all performance requirements against future natural hazards are directly incorporated in the objective function. Finally, the constraints in (2.3) may be incorporated into the definition of admissible design space Φ, which leads to the simplified expression:

$$\boldsymbol{\varphi}^* = \arg\min_{\boldsymbol{\varphi}\in\Phi} C(\boldsymbol{\varphi}) \tag{2.4}$$

For evaluation of (2.2) and optimization (2.4), an approach based on stochastic simulation will be discussed in Section 6.

3. INITIAL COST OF THE FLUID VISCOUS DAMPERS

The initial cost in (2.1) corresponds to the cost of the dampers and it is estimated based on their maximum force capacity for each story $F_{ud,i}$, $i = 1,\ldots,n$, where n is the number of stories of the structure. The force of the damper F_D is given by $F_D = C_D \operatorname{sgn}(\dot{x}_D)\left|\dot{x}_D\right|^{\alpha}$, where C_D is the damper coefficient, $\dot{x}_D$ is the damper velocity and α is the velocity exponent. The design variables of the optimization problem can be, in general, the damper coefficients $C_{D,i}$ and the velocity exponents α_i. The maximum force capacity of a damper $F_{ud,i}$ is typically the maximum force the damper is expected to develop under the maximum credible earthquake defined for the project (TaylorDevices, 2012). Therefore, for a given configuration of $C_{D,i}$ and α_i, the maximum force capacity $F_{ud,i}$ can be calculated by selecting an appropriate reference velocity, which is representative of the velocity corresponding to the maximum credible earthquake considered. Here, the reference velocity is defined as corresponding to a certain probability of exceedance (for a given damper selection) based on the probabilistic seismic hazard description. After the damper capacities have been determined the evaluation of $C_{in}(\boldsymbol{\varphi},\boldsymbol{\theta})$ is relatively straight-forward; it can be performed using data for existing commercial devices.

4. LOSS ESTIMATION METHODOLOGY

For estimating earthquake losses the comprehensive methodology described in (Porter et al., 2001) and in (Goulet et al., 2007) is adopted. In this methodology the nonlinear time-history response of the structure under a given excitation is used to calculate the damage in a component level. For the direct losses, the components of the structure are grouped into n_{as} damageable assemblies. Each assembly consists of components of the structural system that have common characteristics with respect to their vulnerability and repair cost. Such assemblies may include, for example, beams, columns, wall partitions, contents of the building, and so forth. For each assembly $j=1,\ldots,n_{as}$, $n_{d,j}$ different damage states are designated and a fragility function is established for each damage state $d_{k,j}$, $k=1,\ldots,n_{d,j}$. These functions quantify the probability $P_e[d_{k,j}|\mathrm{EDP}_j,\boldsymbol{\varphi},\boldsymbol{\theta}]$ that the component has reached or exceeded its kth damage state, conditional on some engineering demand parameter (EDP_j) which is related to the time-history response of the structure (for example, peak transient drift, peak acceleration, etc.). Damage state 0 is used to denote an undamaged condition. A repair cost $C_{k,j}$ is then assigned to each damage state, which corresponds to the cost needed to repair the component back to the undamaged condition. The expected losses in the event of the earthquake are given by:

$$L(\boldsymbol{\varphi},\boldsymbol{\theta}) = \sum_{j=1}^{n_{as}} \sum_{k=1}^{n_{d,j}} P[d_{k,j} \mid \boldsymbol{\varphi},\boldsymbol{\theta}] C_{k,j} \tag{4.1}$$

where $P\,[d_{k,j}|\boldsymbol{\varphi},\boldsymbol{\theta}]$ is the probability that the assembly j will be in its kth damage state and the explicit dependence on EDP_j has been dropped since in the framework considered here knowledge of the design and model parameter values leads to estimation of EDP_j. The probability $P\,[d_{k,j}|\boldsymbol{\varphi},\boldsymbol{\theta}]$ may be readily obtained from the information from the fragility curves:

$$\begin{aligned} P[d_{k,j}\,|\,\boldsymbol{\varphi},\boldsymbol{\theta}] &= P_e[d_{k,j}\,|\,\boldsymbol{\varphi},\boldsymbol{\theta}] - P_e[d_{k+1,j}\,|\,\boldsymbol{\varphi},\boldsymbol{\theta}], \\ P[d_{n_d,j}\,|\,\boldsymbol{\varphi},\boldsymbol{\theta}] &= P_e[d_{n_d,j}\,|\,\boldsymbol{\varphi},\boldsymbol{\theta}] \end{aligned} \tag{4.2}$$

5. EXCITATION MODEL

The life-cycle assessment framework discussed here requires development of a probabilistic model of the entire ground motion time history that will adequately describe the uncertainty in future earthquake events. Additionally, for the comprehensive characterization of the seismic hazard consideration of the probability of occurrence of a forward-directivity pulse at the beginning of the velocity time history is required, as such type of excitations, observed in near-fault distances (Somerville, 2003), have caused severe damage in structural systems. Therefore, in this study the potential of pulse occurrence in near-fault ground motions is taken into account, through calculation of the probability of occurrence of this velocity pulse, for specified earthquake and site characteristics (Iervolino and Cornell, 2008, Shahi and Baker, 2011). A stochastic model for pulselike excitations is briefly discussed next: according to it, the high-frequency and long period components of the motion are independently modeled and then combined to form the acceleration time history.

5.1. High-frequency component

For modeling the higher-frequency (>0.1-0.2 Hz) component of ground motions, the point source stochastic method (Boore, 2003) is chosen here. This approach is based on a parametric description of the ground motion's radiation spectrum $A(f;M,r)$, which is expressed as a function of the frequency, f, for specific values of the earthquake magnitude, M, and the closest distance to the rupture surface r. This spectrum consists of many factors which account for the spectral effects from the source (source spectrum) as well as propagation through the earth's crust up to the structural site. The duration of the ground motion is addressed through an envelope function $e(t;M,r)$, which again depends on M and r. These frequency and time domain functions, $A(f;M,r)$ and $e(t;M,r)$, completely describe the model, and their characteristics are provided by predictive relationships that relate them directly to the seismic hazard, i.e. to M and r. More details about them are provided in (Taflanidis et al., 2008, Boore, 2003). In particular, the two-corner point-source model by Atkinson and Silva (Atkinson and Silva, 2000) can be selected for the source spectrum because of its equivalence to finite fault models. The time history (output) for a specific event magnitude, M, and source distance, r, is obtained according to this model by modulating a white-noise sequence $\mathbf{Z}_w = [Z_w(i\Delta t):i=1,2,...,N_T]$ by $e(t;M,r)$ (in the time domain) and subsequently by $A(f;M,r)$ (in the frequency domain). The model parameters consist of the seismological parameters, M and r, describing the seismic hazard, the white-noise sequence $\mathbf{Z}_w$, and the predictive relationships for $A(f;M,r)$ and $e(t;M,r)$.

5.2. Long-period pulse

For describing the pulse characteristics of near-fault ground motions, the simple analytical model developed by Mavroeidis and Papageorgiou is selected (Mavroeidis and Papageorgiou, 2003). According to it, the pulse component of near-fault motions is described through the following expression for the ground motion velocity pulse:

$$V(t) = \frac{A_p}{2}\left[1+\cos\left(\frac{2\pi f_p}{\gamma_p}(t-t_o)\right)\right]\cos\left[2\pi f_p(t-t_o)+\nu_p\right] \quad \text{if} \quad t\in\left[t_o-\frac{\gamma_p}{2f_p},t_o+\frac{\gamma_p}{2f_p}\right] \tag{5.1}$$

$$=0 \quad \text{otherwise}$$

where A_p, f_p, v_p, γ_p and t_o describe the signal amplitude, prevailing frequency, phase angle, oscillatory character (i.e. number of half cycles), and time shift to specify the envelope's peak, respectively. These pulse characteristics can be estimated by predictive relationships that connect them to the seismic hazard of a site. In this study the predictive equations proposed by (Dabaghi et al., 2011) are used. These empirical equations link the pulse parameters to the following earthquake and site characteristics: the type of faulting (strike-slip or non strike-slip), the moment magnitude, M, the shear wave velocity in the top 30m of soil at the site, V_{s30}, the epicentral distance R_{epi}, the closest distance to fault rupture, r, the length of rupture between the fault and the site, s, and the angle between the strike of the fault and the line joining epicenter and the site, θ. Figure 5.1 illustrates the source-to-site parameters r, R_{epi}, θ, s and the rupture length L, for the case that the site is located before (left) and after (right) of the end of the rupture length for a strike-slip fault. The rupture length is estimated by the predictive equation proposed by (Wells and Coppersmith, 1994)

$$\log_{10}(L) = -3.55 + 0.74M + e_L \tag{5.2}$$

where e_L is a prediction error following Gaussian distribution with zero mean and a specified standard deviation. Additionally, since not all the near-fault ground motions exhibit this long period pulse, the probability of occurrence of the velocity pulse is calculated using the predictive equation for strike-slip faults proposed by (Shahi and Baker, 2011)

$$P(pulse \mid r, s) = \frac{1}{1 + e^{(0.642 + 0.167r - 0.075s)}} \tag{5.3}$$

5.3. Near-fault ground motion

The stochastic model for near-fault motions is finally established by combining the above two components through the methodology initially developed in (Mavroeidis and Papageorgiou, 2003). The following procedure describes the final model: apply the point-source stochastic method to generate an acceleration time history; generate a velocity time history for the near-field pulse using (5.1), and shift the pulse in time to coincide with the peak of the envelope $e(t;M,r)$ (this defines the value of the time shift parameter t_o); differentiate the velocity time series to obtain an acceleration time series and subtract its Fourier amplitude from the Fourier amplitude of the time history generated by the point-source stochastic method; construct a synthetic acceleration time history so that its Fourier amplitude is the one corresponding to this difference and its Fourier phase coincides with the phase of the time history generated by the point-source stochastic method; finally, superimpose the latter time history with that of the near-fault pulse.

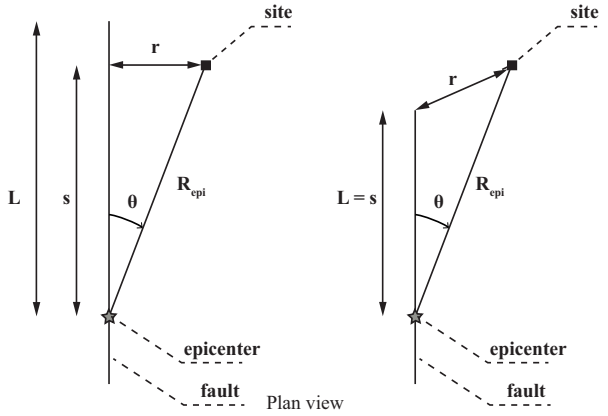

Figure 5.1. Source to site geometry for strike-slip faults

6. LIFE-CYCLE COST OPTIMAL DESIGN: STOCHASTIC ANALYSIS AND OPTIMIZATION

The system, excitation and performance evaluation models described earlier lead to quantification of the performance measure $h(\boldsymbol{\varphi},\boldsymbol{\theta})$, conditional on the values for the model parameters θ and the design configuration $\boldsymbol{\varphi}$. The optimization in (2.4) requires, additionally, the evaluation of the integral corresponding to the objective function. Since the nonlinear models considered are complex and include a large number of uncertain model parameters, this high-dimensional integral cannot be calculated, or even accurately approximated, analytically. An efficient alternative approach is to estimate the integral by *stochastic simulation* (Robert and Casella, 2004). Using a finite number, N, of samples of $\boldsymbol{\theta}$ drawn from some importance sampling density $p_{is}(\boldsymbol{\theta})$, an estimate for (2.2) is given by the *stochastic analysis*:

$$\hat{C}(\boldsymbol{\varphi}) \triangleq \hat{E}[h(\boldsymbol{\varphi},\boldsymbol{\Omega}_N)] = \frac{1}{N}\sum_{i=1}^{N} h(\boldsymbol{\varphi},\boldsymbol{\theta}^i)\frac{p(\boldsymbol{\theta}^i)}{p_{is}(\boldsymbol{\theta}^i)} \tag{6.1}$$

where $\boldsymbol{\Omega}_N = [\boldsymbol{\theta}_1,..., \boldsymbol{\theta}_N]$ is defined as the sample set, and vector $\boldsymbol{\theta}_i$ denotes the sample of the uncertain parameters used in the ith simulation. As $N \to \infty$, then $\hat{C} \to C$ but even for finite, large enough N, (6.1) gives a good approximation for (2.2). The importance sampling density $p_{is}(\boldsymbol{\theta})$ may be used to improve the efficiency of this estimation (Robert and Casella, 2004), by focusing the computational effort on regions the Θ space that contribute more to integrand of the stochastic integral, i.e., by selecting a proposal density that resembles the integrand of (2.2). For problems with a large number of model parameters, such as the application discussed here, choosing efficient importance sampling densities for all components of $\boldsymbol{\theta}$ is challenging; thus it is preferable to formulate importance sampling densities only for the important components of $\boldsymbol{\theta}$, i.e. the ones that have biggest influence on the seismic risk, and use $p_{is}(.) = p(.)$ for the rest. For seismic risk applications the characteristics of the hazard, especially the moment magnitude is generally expected to have the strongest impact on the calculated risk (Taflanidis and Beck, 2009), so selection of importance sampling densities may preliminary focus on it. Finally, using the estimate in (6.1) the optimal design choice is then given by the *optimization under uncertainty*:

$$\boldsymbol{\varphi}^* = \arg\min_{\boldsymbol{\varphi}\in\Phi} \hat{E}[h(\boldsymbol{\varphi},\boldsymbol{\Omega}_N)] \tag{6.2}$$

In this study an exterior sampling approximation (ESA) is adopted for this stochastic design problem. ESA adopts the same stream of random numbers throughout all iterations in the optimization process, thus transforming problem (6.2) into a deterministic system design problem, which can be solved by any appropriate deterministic optimization algorithm. Still, the estimate of the objective function for this optimization involves significant computational cost since N evaluations of the model response are needed for each stochastic analysis. This feature make the optimization problem challenging. An efficient search technique, belonging in the greater family of costly global optimization, CGO, algorithms (Holmstrom et al., 2009), is used which utilizes response surface approximations for the objective function. For implementing this approach the powerful optimization toolbox TOMLAB (Holmstrom et al., 2009) is adopted here.

7. ILLUSTRATIVE EXAMPLE

For the illustrative example, a three-story reinforced concrete office building with nonlinear fluid viscous dampers is considered. The dimension of the building is 32 x 36 m and the height of each story is 4.0 m. The shear wave velocity in the top 30m of the soil at the site, V_{s30}, is assumed to be 310 m/sec, which corresponds to generic soil conditions, while the type of the fault is assumed to be strike –slip. The design variables in this problem correspond to the damper coefficients in each story $C_{D,i}$, i = 1,2,3. The damper capacities $F_{ud,i}$ are calculated by assuming that the velocity exponents for each α_i are equal to 0.5, a value which corresponds to highly nonlinear behavior of the dampers, and that the reference velocity discussed in Section 3 is equal to the one that has 1% probability of exceedance.

7.1. Structural and excitation models

A planar frame model (illustrated in Figure 7.1) with peak oriented hysteretic behavior and deteriorating stiffness and strength is assumed. The median value for the lumped masses of all the stories are $[m_i]$ = [976, 932, 887] metric tons, i=1,2,3. All three masses are assumed uncertain, following a log-normal distribution with coefficient of variation (c.o.v.) 10%. The initial inter-story stiffnesses k_i of all the stories are parameterized by $k_i = \hat{k}_i \theta_{k,i}$, i=1,2,3, where $[\hat{k}_i]$ = 789.02[1.00, 0.85, 0.70] MN/m are the most probable values and $\theta_{k,i}$ are nondimensional uncertain parameters, assumed to be correlated Gaussian variables with mean value one and covariance matrix with variances 0.10 for all the floors and correlation coefficients 0.5 between adjacent floors and 0.2 between first and third floor. For each story, the post-yield stiffness coefficients a_i, stiffness deterioration coefficient β_i, over-strength factor γ_i, ductility coefficient μ_i, and yield displacement $\delta_{y,i}$ have median values 0.1, 0.2, 4 and 0.5% of story height, respectively (see Figure 7.1 for proper definition of some of these parameters). All these parameters are treated as independent log-normal variables with c.o.v. 10%. Additionally, a residual strength is assumed equal to 10% of the maximum strength. The structure is assumed to be modally damped. The damping ratios for all modes are treated as log-normal variables with median values 5% and c.o.v. 30%.

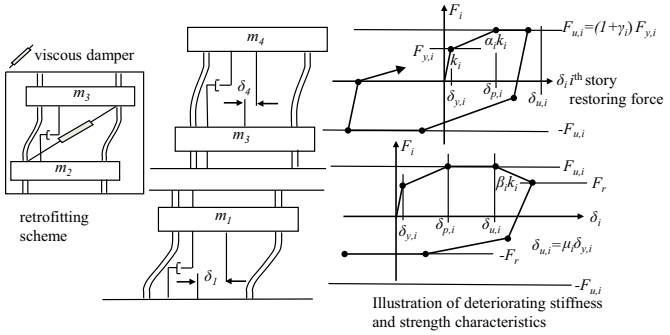

Figure 7.1. Structural model

Seismic events are assumed to occur following a Poisson distribution and so are independent of previous occurrences. The uncertainty in moment magnitude M is modeled by the Gutenberg-Richter relationship truncated on the interval $[M_{min}, M_{max}]$ = [5.0, 8.0], leading to the PDF and expected number of events per year given, respectively, by (Kramer, 2003):

$$p(M) = \frac{b_M \exp(-b_M M)}{\exp(-b_M M_{\min}) - \exp(-b_M M_{\max})}$$
$$v = \exp(a - bM_{\min}) - \exp(a - bM_{\max}) \tag{7.1}$$

Only events with magnitude greater than M>5.0 are considered since earthquakes with smaller magnitude are not expected to lead to significant damage to the structure and thus will not contribute significantly to the expected life-cycle cost. The regional seismicity factors are selected as b=0.9log$_e$(10) and a=4.35log$_e$(10), leading to v=0.25. Following discussion of Section 6 importance sampling density was used only for M; it was used a truncated on the interval $[M_{min}, M_{max}]$ Gaussian PDF with mean value 6.8 and standard deviation 1. For the uncertainty in the event location and orientation with respect to the fault, the epicentral distance R_{epi}, for the earthquake events is assumed to follow a log-normal distribution with median 22 km and c.o.v. 0.4, whereas the angle between the strike of the fault and the line joining epicenter and the site, θ, is assumed to follow a Beta distribution with parameters a_{beta}=1.73 and b_{beta}=4.07. The prediction error e_L for the rupture length is treated as a Gaussian variable with zero mean and standard deviation 0.23. Parameters r and s can be derived from the source to site geometry as depicted in Figure 5.1.

7.2. Expected life-cycle cost

The initial cost in (2.1) corresponds to the cost of the dampers and it is estimated based on their maximum force capacity $F_{ud,i}$, as $C_{init,i}(\boldsymbol{\varphi}) = \$\,(0.77(\mathrm{F}_{ud,i})^{1.207} + 2806)$. This approximate cost equation has been derived by fitting to a curve of some commercially-available dampers (TaylorDevices, 2012). The constant term in the above equation corresponds to installation cost of the dampers. The lifetime cost corresponds to the present value of the losses from future seismic events which is calculated by $C_{lif}(\boldsymbol{\varphi},\boldsymbol{\theta}) = L(\boldsymbol{\varphi},\boldsymbol{\theta})\left[vt_{life}\left(1-e^{-r_d t_{life}}\right)\Big/ r_d t_{life}\right]$, where r_d is the discount rate (assumed here 2.5%), t_{life} is the lifetime of the structure (taken 60 years) and $L(\boldsymbol{\varphi},\boldsymbol{\theta})$ is the expected cost given the occurrence of an earthquake event. The earthquake damage and loss are calculated assuming that after each event the structure is quickly restored in its undamaged state.

Table 7.1. Characteristics of fragility functions and expected repair cost for each story

$d_{k..j}$	x_m	b_m	n_{el}	\$/n_{el}
		Structural components		
1(light)	$1.2\delta_{y,i}$	0.20	42	2000
2(moderate)	$(\delta_{y,i}+\delta_{p,i})/2$	0.35	42	9625
3(significant)	$\delta_{p,i}$	0.40	42	18200
4(severe)	$\delta_{u,i}$	0.40	42	21600
5(collapse)	5%	0.50	42	34300
		Contents		
1(damage)	0.70*g*	0.30	50	500
		Partitions		
1(small cracks)	0.25%	0.70	640 m^2	3.14
2(extensive cracks)	0.6%	0.50	640 m^2	48.44
3(severe damage)	1.4%	0.40	640 m^2	107.64
		Acoustical ceiling		
1(some tiles fallen)	0.55*g*	0.40	500 m^2	5.38
2(extensive tile fallout)	1.00*g*	0.40	500 m^2	25.79
		Paint		
1(damage)	0.33%	0.2	640 m^2	21.53

The earthquake losses $L(\boldsymbol{\varphi},\boldsymbol{\theta})$ are calculated according to the methodology presented in Section 4. Each fragility function is a conditional cumulative log-normal distribution with median x_m and standard deviation b_m, as described Table 7.1, which also presents the expected cost per element \$/n_{el}, where n_{el} corresponds to the number of elements that belong to each damageable assembly in each direction of each of each floor. For structural components, partitions and paint the maximum interstory drift is used as the EDP, while for the rest the maximum story absolute acceleration is used as the EDP. The fragility curves used are similar to the ones selected in (Goulet et al., 2007) for all damageable subassemblies except for the structural components. For the latter the fragility curves are chosen with respect to the characteristics of the backbone curve for the restoring force in each story. Therefore, a direct link is established between the fragility curves and the stiffness and strength characteristics of the structural model, considering their associated uncertainties.

7.3. Results and discussion

The number of evaluations, N, of the model response for each damper configuration is selected to be N=2000. It is noted that approximately only 22% of the generated sample excitation time-histories exhibit the long period velocity pulse, as a consequence of the incorporation in the excitation model of the probability of occurrence of a pulse (5.3), given the earthquake and site characteristics. The damper coefficients in each floor are the three design variables $\boldsymbol{\varphi} = [C_{D,i}: i = 1,2,3]$. The initial design space for each variable is set to [12 20] MN/(m/sec)$^{0.5}$ for $C_{D,1}$, [8.4 14] MN/(m/sec)$^{0.5}$ for $C_{D,2}$ and [6 10] MN/(m/sec)$^{0.5}$ for $C_{D,3}$. Table 7.2 presents cumulative results from the optimization, which includes the optimal design configuration $\boldsymbol{\varphi}^*$, the maximum force capacities of the dampers for this

configuration, the total life cycle cost $C(\boldsymbol{\varphi}^*)$, the upfront cost of the dampers $C_{init}(\boldsymbol{\varphi}^*)$ and the repair cost for the lifetime of the structure $C_{lif}(\boldsymbol{\varphi}^*,\boldsymbol{\theta})$, as well as the total life cycle cost for the structure without retrofitting ($C_{D,i} = 0$). The results illustrate the fact that retrofitting of the structure with fluid viscous dampers leads to a significant reduction of the total life-cycle cost (≈ 22% of the cost of the structure without dampers). The latter result verifies that the addition of the damper devices can significantly reduce the interstory drifts and absolute accelerations of the structural system and consequently minimize the damage to the structural and non-structural components.

Table 7.2. Optimization results; the units for $C_{D,i}$ are kN/(m/sec)$^{0.5}$

Case		$\boldsymbol{\varphi}^*$	$F_{ud,i}$ (kN)	$\hat{C}(\boldsymbol{\varphi}^*)$ ($)	$C_{init}(\boldsymbol{\varphi}^*)$ ($)	$C_{lif}(\boldsymbol{\varphi}^*,\boldsymbol{\theta})$ ($)
Dampers	$C_{D,1}$	18407.72	7123	115710	79588	36119
	$C_{D,2}$	12189.28	4380			
	$C_{D,3}$	6528.64	2014			
No dampers		-	-	522,030	0	522,030

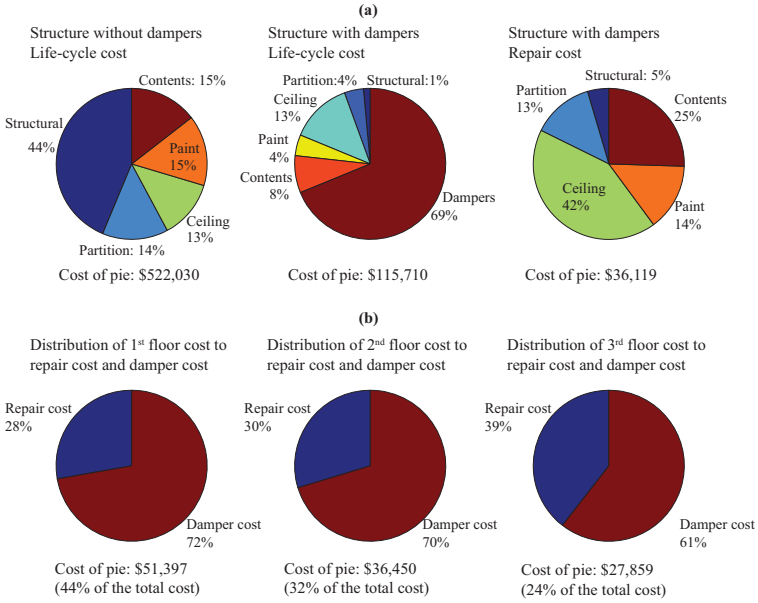

Figure 7.2. (a) Details about life-cycle cost; **(b)** Distribution of life-cycle cost to the different floors

Figure 7.2 (a) reports the distribution of the life-cycle cost and the lifetime repair cost for both the structure with and without the fluid viscous dampers. It can be observed that the retrofitting of the structure changes significantly the distribution of the lifetime repair cost over the different components, since the addition of the dampers increases considerable the relative importance of the acceleration sensitive components, while it reduces the importance of the drift sensitive components. The latter behavior is expected, since the addition of the dampers results in the increase of the amount of energy dissipated by the system and consequently to the reduction of the interstory drifts. It is interesting to note the significant reduction of the contribution to the cost related with the structural components, which is an indication of the efficiency of the retrofitting of the structure. Figure 7.2(b) illustrates the distribution of the lifetime repair cost and the cost of the dampers over the three stories of the retrofitted building.

Additionally, the contribution of the cost of each floor to the total life-cycle cost is presented. The contribution of the damper cost to the total cost of each floor slightly decreases from the 1st to the 2nd floor, whereas its reduction is more evident for the 3rd floor. This trend is expected and can be attributed to the fact that in general the shear demands are higher in the lower floors; thus dampers with higher force capacities are required in order to dissipate the seismic energy induced in the lower floors.

8. CONCLUSIONS

The robust (with respect to structural and excitation uncertainties) optimal performance-based design of fluid viscous dampers for a three-story concrete structure was discussed in this study. The life-cycle cost was adopted as the performance objective. The basis of the suggested approach is a probabilistic framework that explicitly addresses all sources of uncertainty related either to future excitations or to the structural configuration, by appropriate probability models. In this setting the expected life-cycle cost is ultimately expressed through a multi-dimensional integral and stochastic simulation is suggested for its evaluation. Though robust, this choice makes the associated design-optimization challenging, as it involves a large computational burden. To alleviate this burden, an efficient algorithm belonging in the greater family of Costly Global Optimization (CGO) search techniques is adopted here. An illustrative example was presented that considered the optimal design of nonlinear fluid viscous dampers for minimizing the expected life-cycle cost of a three-story concrete structure. The addition of the dampers was shown to significantly improve the structure's performance by reducing its life-cycle cost.

REFERENCES

Atkinson, G. M. & Silva, W. (2000). Stochastic modeling of California ground motions. *Bulletin of the Seismological Society of America,* **90,** 255-274.

Boore, D. M. (2003). Simulation of ground motion using the stochastic method. *Pure and Applied Geophysics,* **160,** 635-676.

Dabaghi, M., Rezaeian, S. & Der Kiureghian, A. (2011). Stochastic simulation of near-fault ground motions for specified earthquake and site chracteristics. *11th International Conference on Applications of Statistics and Probability in Civil Engineering.* Zurich, Switzerland.

Goulet, C. A., Haselton, C. B., Mitrani-Reiser, J., Beck, J. L., Deierlein, G., Porter, K. A. & Stewart, J. P. (2007). Evaluation of the seismic performance of code-conforming reinforced-concrete frame building-From seismic hazard to collapse safety and economic losses. *Earthquake Engineering and Structural Dynamics,* **36,** 1973-1997.

Holmstrom, K., Goran, A. O. & Edvall, M. M. (2009). User's guide for TOMLAB 7*,* San Diego, CA, Tomlab Optimization Inc. www.tomopt.com/tomlab/.

Iervolino, I. & Cornell, C. A. (2008). Probability of occurrence of velocity pulses in near-source ground motions. *Bulletin of the Seismological Society of America,* **98,** 2262-2277.

Jaynes, E. T. (2003). Probability Theory: The logic of science*,* Cambridge, UK, Cambridge University Press.

Kramer, S. L. (2003). Geotechnical earthquake engineering, Prentince Hall.

Mavroeidis, G. P. & Papageorgiou, A. P. (2003). A mathematical representation of near-fault ground motions. *Bulletin of the Seismological Society of America,* **93,** 1099-1131.

Porter, K. A., Kiremidjian, A. S. & Legrue, J. S. (2001). Assembly-based vulnerability of buildings and its use in performance evaluation. *Earthquake Spectra,* **18,** 291-312.

Robert, C. P. & Casella, G. (2004). Monte Carlo statistical methods*,* New York, NY, Springer.

Shahi, S. K. & Baker, J. W. (2011). An Empirically Calibrated Framework for Including the Effects of Near-Fault Directivity in Probabilistic Seismic Hazard Analysis. *Bulletin of the Seismological Society of America,* **101,** 742-755.

Somerville, P. G. (2003). Magnitude scaling of the near fault rupture directivity pulse. *Physics of the Earth and Planetary Interiors,* **137,** 201-212.

Taflanidis, A. A. & Beck, J. L. (2009). Life-cycle cost optimal design of passive dissipative devices *Structural Safety,* **31,** 508-522.

Taflanidis, A. A., Scruggs, J. T. & Beck, J. L. (2008). Probabilistically robust nonlinear design of control systems for base-isolated structures. *Journal of Structural Control and Health Monitoring,* **15,** 697-719.

TaylorDevices. (2012). *RE: Personal communication.*

Wells, D. L. & Coppersmith, K. J. (1994). New empirical relationships among magnitude, rupture length, rupture width, rupture area, and surface displacement. *Bulletin of the Seismological Society of America,* **84,** 974-1002.